Water-soluble Ru(II)- and Ru(III)-halide-PTA complexes (PTA = 1,3,5-triaza-7-phosphaadamantane): chemical and biological properties

F. Battistin,[a†] F. Scaletti,[b†] G. Balducci,[a] S. Pillozzi,[c] A. Arcangeli,[c] L. Messori,[b*] E. Alessio,[a*]

[a] Department of Chemical and Pharmaceutical Sciences, University of Trieste, Via L. Giorgieri 1, 34127 Trieste, Italy. Email: alessi@units.it.

[b] Department of Chemistry "Ugo Schiff", University of Florence, Via della Lastruccia 3-13, 50019 Sesto Fiorentino, Florence, Italy. Email: luigi.messori@unifi.it

[c] Department of Experimental and Clinical Medicine, University of Florence, Viale G.B. Morgagni 50, 50134 Florence, Italy.

[†] These Authors contributed equally to the work.

Abstract

Four structurally related Ru(II)-halide-PTA complexes, of general formula *trans*- or *cis*-$[Ru(PTA)_4X_2]$ (PTA = 1,3,5-triaza-7-phosphaadamantane, X = Cl (**1**, **2**), Br (**3**, **4**), were prepared and characterized. Whereas compounds **1** and **2** are known, the corresponding bromo derivatives **3** and **4** are new. The Ru(III)-PTA compound *trans*-$[RuCl_4(PTAH)_2]Cl$ (**5**, PTAH = PTA protonated at one N atom), structurally similar to the well-known Ru(III) anticancer drug candidates (Na)*trans*-$[RuCl_4(ind)_2]$ (NKP-1339, ind = indazole) and (Him)*trans*-$[RuCl_4$(dmso-S)(im)] (NAMI-A, im = imidazole), was also prepared and similarly investigated. Notably, the presence of PTA confers to all complexes an appreciable solubility in aqueous solutions at physiological pH. The chemical behavior of compounds **1** – **5** in water and in physiological buffer, their interactions with two model proteins – cytochrome c and ribonuclease A – as well as with a single strand oligonucleotide (5'-CGCGCG-3'), and their *in vitro* cytotoxicity against a human colon cancer cell line (HCT-116) and a myeloid leukemia (FLG 29.1) were investigated. Upon dissolution in the buffer, sequential halide replacement by water molecules was observed for complexes **1** – **4**, with relatively slow kinetics, whereas the Ru(III) complex **5** is more inert. All tested compounds manifested moderate antiproliferative properties, the *cis* compounds **2** and **4** being slightly more active than the *trans* ones (**1** and **3**). Mass spectrometry experiments evidenced that all complexes exhibit a far higher reactivity toward the reference oligonucleotide than toward model proteins. The chemical and biological profiles of compounds **1** – **5** are compared to those of established ruthenium drug candidates in clinical development.

1. Introduction

The interest in ruthenium derivatives – both coordination and organometallic compounds – as potential anticancer drugs has grown almost exponentially in the last 20 years and does not deserve much introduction [1-10].

Since several years the cage-like monodentate phosphane 1,3,5-triaza-7-phosphaadamantane (PTA, Figure 1) has been widely used as a co-ligand in the design of organometallic Ru(II) anticancer compounds. The half-sandwich RAPTA-type compounds $[RuCl_2(\eta^6\text{-arene})(PTA)]$ (RAPTA = Ruthenium-Arene PTA, Figure 1) developed by the group of Dyson are the most well-known [11-17], but other Ru(II) compounds containing PTA have been investigated for their anticancer [18-23] or DNA-binding [24-26] properties.

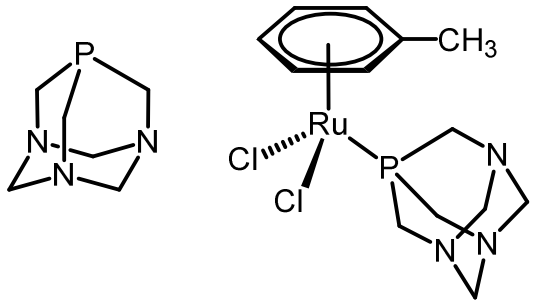

Figure 1. The PTA ligand (left) and a representative example of the RAPTA compounds (RAPTA-T, right).

PTA is an amphiphilic neutral ligand of moderate steric demand (cone angle 103°) that dissolves in several organic solvents and – most importantly – is characterized by a high solubility in water (ca. 235 g/L) by virtue of H-bonding to the tertiary amine nitrogens [27,28]. It typically binds strongly to metal ions through the P atom in a monodentate fashion, imparting excellent water solubility to its complexes [27,28]. PTA has good σ- and π-bonding abilities and, even though it has been defined as an air-stable, water-soluble version of PMe_3 [29], spectroscopic and structural data suggest that it is closer to $P(OMe)_3$ rather than PMe_3 in terms of coordinating properties [27,28]. The solubility properties PTA-metal complexes were considered to be potentially very useful not only in homogeneous aqueous-organic biphasic catalysis [30-35], but also for the development of new metal anticancer drugs. In fact, in this context metal complexes containing PTA as co-ligand are anticipated to have good solubility in water for ease of *in vitro* investigation and *in vivo* administration, whereas maintaining sufficient lipophilicity to cross cell membranes and hence enter

cancer cells. In addition, at moderately acidic pH (the pK_a of PTA is 5.89 [36]) one of the three N atoms of PTA is selectively protonated to generate PTAH. This feature was originally considered important for improving the selectivity of RAPTA compounds towards hypoxic cells of solid tumors that have slightly lower pH than normal cells (protonation of coordinated PTA inside the cell might lead to trapping the resulting cationic complex) [37]. However, this working hypothesis was later abandoned, since the pK_a of PTA typically drops to ca. 3 when bound to ruthenium [21,38], thus well below the pH of cancer cells. Finally, PTA appears to be a quite safe molecule in terms of toxicity.

Given these premises, we were surprised at realizing that even though PTA has been extensively used as co-ligand in many Ru half-sandwich anticancer compounds, no investigation has been yet performed on the ruthenium-halide complexes of PTA, i.e. on complexes in which PTA is the main ligand.

Two neutral chloro Ru(II)-PTA isomers, namely *trans*-[$RuCl_2(PTA)_4$] (**1**) and *cis*-[$RuCl_2(PTA)_4$] (**2**) are known since several years and can be obtained in good yield upon treatment of hydrated $RuCl_3$ with excess PTA [39-42]. In this work we report the preparation and characterization of the corresponding – and new – bromo derivatives, *trans*-[$RuBr_2(PTA)_4$] (**3**) and *cis*-[$RuBr_2(PTA)_4$] (**4**), and of the Ru(III) complex *trans*-[$RuCl_4(PTAH)_2$]Cl (**5**), structurally similar to well-known Ru(III) anticancer drug candidates (Na)*trans*-[$RuCl_4(ind)_2$] (NKP-1339, ind = indazole) and (Him)*trans*-[$RuCl_4$(dmso-S)(im)] (NAMI-A, im = imidazole) [1-10]. The chemical behavior of compounds **1** – **5** in water and in physiological buffer, their interactions with two model proteins – cytochrome c (cyt c) and ribonuclease A (RNase A) – as well as with a single strand reference oligonucleotide (5'-CGCGCG-3', ODN4), and their in vitro cytotoxicity against a human colon cancer cell line (HCT-116) and a myeloid leukemia (FLG 29.1) are also reported.

2. Experimental procedures

2.1 Materials and methods

All chemicals were purchased from Sigma-Aldrich and used as received. Solvents were of reagent grade. The compounds *trans*-[$RuCl_2(PTA)_4$] (**1**), *cis*-[$RuCl_2(PTA)_4$] (**2**), and [$(dmso)_2H$]*trans*-[$RuCl_4$(dmso-S)$_2$] were prepared as described in the literature [39-43]. Hydrated $RuCl_3$ was a gift from BASF Italia Srl, whereas hydrated $RuBr_3$ was purchased from Strem Chemicals.

Horse heart cytochrome c (cyt c) (C7752), Ribonuclease A (RNase A) from bovine pancreas type XII-A (RNase 055K7695), as well as all the chemicals for the various buffer solutions were purchased from Sigma. Single strand oligonucleotide ODN4 (5'-CGCGCG-3') was purchased from

Jena Bioscence (Oligo4_4, 5073). All the chemicals and proteins were used as received without further purification, and the solutions were prepared with deionized water produced by a Millipore system.

Mono- (^{1}H (400 or 500 MHz), ^{13}C (125.7 MHz), ^{31}P (161 or 202 MHz)) and bi-dimensional (^{1}H-^{1}H COSY and ^{1}H-^{13}C HSQC) NMR spectra were recorded at room temperature on a JEOL Eclipse 400FT or on a Varian 500 spectrometer. ^{1}H and ^{13}C chemical shifts were referenced to the peak of residual non-deuterated solvent (δ = 7.26 and 77.16 for $CDCl_3$) or were measured relative to the internal standard DSS (δ = 0.00) for D_2O. ^{31}P chemical shifts were measured relative to external 85% H_3PO_4 at 0.00 ppm. ESI mass spectrometry measurements were performed on a Perkin-Elmer APII spectrometer on an Orbitrap high-resolution mass spectrometer (Thermo Scientific, San Jose, CA, USA) equipped with a conventional ESI source. UV-vis spectra were obtained on an Agilent Cary 60 spectrophotometer, using 1.0 cm path-length quartz cuvettes (3.0 mL). Elemental analyses were performed in the analytical laboratories of the Department of Chemistry of the University of Bologna. A home-made LED apparatus was used for performing the photochemical reactions. Briefly, it consists of a plastic-coated cylindric well capable of hosting an NMR tube or a test-tube (Ø = 20 mm, h = 110 mm). The inside of the apparatus is lined with four pairs of LED stripes, each containing five LEDs of the same color that emit in a narrow spectral range (ca. 10 nm). LED stripes of the same color are located opposite to each other. One or more colors can be activated at the same time, and the LED emission power can be regulated from 1 to 40 mW. The blue LEDs (λ = 470 nm) were used in this case.

2.2 Synthesis and characterization of ruthenium compounds

***trans*-[RuBr$_2$(PTA)$_4$] (3).** $RuBr_3 \cdot 3H_2O$ (60.0 mg, 0.15 mmol) was partially dissolved in 7 mL of ethanol. A slight excess of PTA (96.55 mg, 0.615 mmol) was added and the mixture was refluxed for 3 h. A clear solution was obtained within 1 h from which a dark red solid began to form. It was eventually removed by filtration and washed with ethanol. The solid was treated on the filter with chloroform (*ca*. 10 mL) to obtain an orange solution. A small amount of grey solid that remained undissolved on the filter was discarded. The solvent was completely removed by rotary evaporation, affording pure **3**, according to ^{1}H and ^{31}P NMR spectra (Yield: 93.9 mg, 68%). X-ray quality crystals of **3** were obtained by slow diffusion of diethyl ether into a chloroform solution of the complex. Elemental analysis for the raw material: calcd for $[C_{24}H_{48}N_{12}Br_2P_4Ru \cdot 5H_2O]$ (M_W: 979.48): C, 29.43; H, 5.97; N, 17.16. Found: C, 29.57; H, 6.10; N, 17.09. ^{1}H NMR (D_2O), δ (ppm): 4.61 (br s, 24H, NC*H*$_2$N), 4.40 (br s, 24H, NC*H*$_2$P). ^{13}C NMR from the HSQC spectrum (D_2O), δ (ppm): 70.5 (N*C*H$_2$N), 51.9 (N*C*H$_2$P). ^{31}P-NMR (D_2O), δ (ppm): –54.5 (s). ^{1}H NMR ($CDCl_3$), δ

(ppm): 4.60, 4.55 (ABq 24H, NCH_2N, J_{AB} 13.2 Hz), 4.46 (br s, 24H, NCH_2P). ^{13}C NMR from the HSQC spectrum ($CDCl_3$), δ (ppm): 73.5 (NCH$_2$N), 54.0 (NCH$_2$P). ^{31}P NMR ($CDCl_3$), δ (ppm): –56.5 (s). ESI mass spectrum (*m*/*z*): 811.12 $(M - Br)^+$, calcd 811.129; 733.97 $(M - PTA + H^+)^+$, calcd 733.32.

***cis*-[RuBr$_2$(PTA)$_4$] (4).** *trans*-$RuBr_2(PTA)_4$ (50.0 mg, 0.056 mmol) was dissolved in 5 mL of water and irradiated with blue light (λ = 470 nm, 40 mW) for 2.30 h. The orange solution turned to yellow within 1 h. Complete removal of the solvent by rotary evaporation afforded pure **4**, according to ^{1}H and ^{31}P NMR spectra, as a yellow solid (Yield: 48.0 mg, 96%). X-ray quality crystals of **4** were obtained by slow diffusion of acetone into a water solution of the complex. Elemental analysis calcd for [$C_{24}H_{48}N_{12}Br_2P_4Ru\cdot 5H_2O$] ($M_W$: 979.48): C, 29.43; H, 5.97; N, 17.16. Found: C, 29.55; H, 6.11; N, 17.07.^{1}H NMR (D_2O + exc. NaBr, see text), δ (ppm): 4.70 (m, 24H, NCH_2N), 4.56 (br s, 12H, NCH_2P), 4.23 (br s, 12H, NCH_2P). ^{31}P NMR (D_2O + exc. NaBr, see text), δ (ppm): –24.1 (t, 2P, $^2J_{P\text{-}P}$ = 28.2 Hz, PTA *trans* to Br), –64.7 (t, 2P, $^2J_{P\text{-}P}$ = 28.2 Hz, mutually *trans* PTAs). ^{1}H NMR ($CDCl_3$), δ (ppm): 4.54 (br s, 12H, NCH_2P), 4.50 (m, 24H, NCH_2N), 4.12 (br s, 12H, NCH_2P). ^{13}C NMR from the HSQC spectrum ($CDCl_3$), δ (ppm): 73.0 (NCH$_2$N), 59.2 (NCH$_2$P), 55.4 (NCH$_2$P). ^{31}P NMR ($CDCl_3$), δ (ppm): –27.0 (t, 2P, $^2J_{P\text{-}P}$ = 27.4 Hz , PTA *trans* to Br), –67.3 (t, 2P, $^2J_{P\text{-}P}$ = 27.4 Hz, mutually *trans* PTAs). ESI mass spectrum (*m*/*z*): 811.12 $(M - Br)^+$, calcd 811.129.

***trans*-[RuCl$_4$(PTAH)$_2$]Cl (5).** [(dmso)$_2$H]*trans*-[$RuCl_4$(dmso-S)$_2$] (150.0 mg, 0.27 mmol) [43] was dissolved in 15 mL of methanol, obtaining an orange solution. 0.500 μL of 37% aqueous HCl and two equivalents of PTA (84.8 mg, 0.54 mmol) were added; a brown solid began to precipitate immediately. The mixture was stirred for 1 h and then the solid was collected by filtration, washed with methanol and diethyl ether and dried *in vacuo*. The solid was dissolved in 4.5 mL of water at reflux. Abundant small crystals of **5**, suitable for X-ray diffraction, were obtained upon allowing the solution to cool down to room temperature. The crystals were filtered, washed with a small amount of water and dried *in vacuo* (yield: 115.8 mg, 72%). Elemental analysis calcd for [$C_{12}H_{26}N_6Cl_5P_2Ru\cdot 2H_2O$] ($M_W$: 630.67): C 22.85; H 4.79; N 13.33. Found: C 23.36; H 4.51; N 13.05 ^{1}H NMR (D_2O), δ (ppm): 0.37 (br s, 12H), –1.17 (br s, 12H). ESI mass spectrum: 400.7 *m*/*z* $(M - PTA)^-$, calcd 400.0.

2.3 *X-ray diffraction*

Data collections were performed at the X-ray diffraction beamline (XRD1) of the Elettra Synchrotron of Trieste (Italy), with a Pilatus 2M image plate detector. Complete datasets were collected at 100 K (295 K for compound **5**, since the crystals cracked at low temperature) with a

monochromatic wavelength of 0.700 Å through the rotating crystal method. The crystals were dipped in paratone-N and mounted on the goniometer head with a nylon loop. The diffraction data were indexed, integrated and scaled using XDS [44]. The structures were solved by direct methods using SIR2014 [45], Fourier analyzed and refined by the full-matrix least-squares methods based on F^2 implemented in SHELXL-2014 [46]. The Coot program was used for modeling [47]. Anisotropic thermal motion modeling was then applied to all atoms. Hydrogen atoms were included at calculated positions with an isotropic temperature factor equal to 1.2 (1.5 for disordered water molecules) times the equivalent isotropic temperature factor of the atom to which they were bonded. CCDC-1429123 (**3**), 1429111 (**4**), 1429110 (5). Essential crystal and refinement data, together with selected bond distances and angles, are reported in the SI.

2.4 Spectrophotometric studies

To assess the stability of the compounds in physiological like conditions, spectrophotometric studies were performed by a Varian Cary 50 Bio UV–vis spectrophotometer. Freshly prepared concentrated solutions (10^{-2} M for compounds **1**–**4**, 10^{-4} M for compound **5**) of each compound dissolved in milliQ water were diluted in phosphate buffer (PB, 10 mM phosphate, pH 7.4). The concentration of each compound in the final sample was 3×10^{-5} M. The resulting solutions were monitored by collection of the electronic spectra for 24 h at room temperature.

2.5 Interactions with biomolecules

Ruthenium complex–protein/oligonucleotide adducts were prepared starting from a solution of each model protein at a concentration of 10^{-4} M in 20 mM ammonium acetate buffer, pH 7.4, or from a 10^{-4} M solution of ODN4 in milliQ water. Then, the ruthenium complex was added (3:1 metal-to-protein/oligonucleotide ratio) to the solution and the mixture was incubated at 37 °C for 24 h, using Thermoblock (Falc, TD15093). Protein samples were analyzed after a 20-fold dilution with milliQ water (the final concentration of the protein was 5 μM), while ODN4 samples were diluted with a mixture of 50% milliQ water and 50% MeOH to a final concentration of 10 μM. ESI-MS spectra were recorded by direct introduction of the sample at a flow rate of 5 μL/min into an Orbitrap high-resolution mass spectrometer (Thermo Scientific, San Jose, CA, USA) equipped with a conventional ESI source. The working conditions for ruthenium complex-protein adducts were as follows: spray voltage 3.1 kV, capillary voltage 45 V and capillary temperature 220 °C. The sheath and the auxiliary gasses were set at 17 (arbitrary units) and 1 (arbitrary unit), respectively. For acquisition, Xcalibur 2.0 (Thermo Scientific) was used and monoisotopic and average deconvoluted masses were obtained by using the integrated Xtract tool. For spectrum acquisition, a nominal

resolution (at m/z 400) of 100,000 was used. ESI-MS spectra of the ruthenium complex-ODN adducts were recorded in negative ion mode. The working conditions were as follows: spray voltage 4.5 kV, capillary voltage –10 V and capillary temperature 270 °C. The sheath gas was set at 10 (arbitrary units) whereas auxiliary gas was kept at 5 (arbitrary units).

2.5 Cellular studies

Cell cultures. HCT-116 (human colon cancer) and FLG 29.1 (human myeloid leukemia) cell lines were maintained in RPMI 1640 medium supplemented with 2 mM L-glutamine, 10% bovine calf serum (HyClone) and maintained at 37°C in a humidified atmosphere in 5% CO_2 in air.

Pharmacology experiments. Cells were seeded in a 96-well flat-bottomed plate (Corning-Costar, Corning, NY, USA) at a cell density of 10^4 cells per well in RPMI complete medium. Each ruthenium compound was added at final concentrations of 200 μM, 100 μM, 50 μM, 10 μM, and 2 μM. After 24 h, viable cells (determined by Trypan blue exclusion) were counted in triplicate using a haemocytometer. Each experimental point represents the mean of four samples carried out in three separate experiments.

Trypan blue assay. Cells viability was assessed by the Trypan blue exclusion assay. In brief, 10 μl of 0.4% trypan blue solution was added to 10 μl cell suspension in culture medium. The suspension was gently mixed and transferred to a haemocytometer. Viable and dead cells were identified and counted under a light microscope. Blue cells failing to exclude dyes were considered nonviable, and transparent cells were considered viable. The percentage of viable cells was calculated on the basis of the total number of cells (viable plus nonviable). The IC_{50} value (i.e. the dose that caused apoptosis of 50% of cells) was calculated by fitting the data points (after 24 h of incubation) with a sigmoidal curve using Calcusyn software (Biosoft).

3. Results and Discussion

The present study is focused on four structurally related Ru(II)-PTA complexes of general formula *trans*- or *cis*-[Ru(PTA)$_4$X$_2$] (PTA = 1,3,5-triaza-7-phosphaadamantane, X = Cl (**1**, **2**), Br (**3**, **4**)), and on the Ru(III)-PTA compound *trans*-[RuCl$_4$(PTAH)$_2$]Cl (**5**, PTAH = PTA protonated at one N atom). Their structures are synoptically represented in Figure 2.

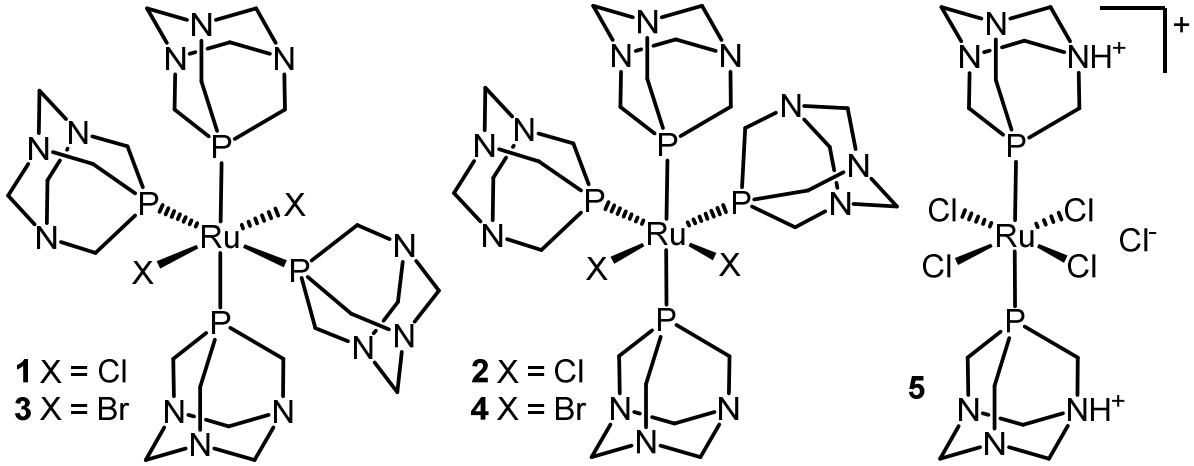

Figure 2. Schematic structures of compounds **1** – **5**.

3.1 Synthesis and chemical characterization

The preparation of the new bromo derivatives *trans*-[RuBr$_2$(PTA)$_4$] (**3**) and *cis*-[RuBr$_2$(PTA)$_4$] (**4**) was performed following a procedure very similar to that reported in the literature for the corresponding chloro isomers **1** and **2**, respectively [39-42], using hydrated RuBr$_3$ rather than RuCl$_3$ as starting material. In summary, treatment of RuBr$_3$·3H$_2$O with excess PTA in refluxing ethanol afforded in high yield *trans*-[RuBr$_2$(PTA)$_4$] (**3**), that precipitates spontaneously. This kinetic product was quantitatively transformed into the thermodynamically stable *cis* isomer *cis*-[RuBr$_2$(PTA)$_4$] (**4**) by irradiating an aqueous solution with blue light (λ = 470 nm) for 2.5 h.

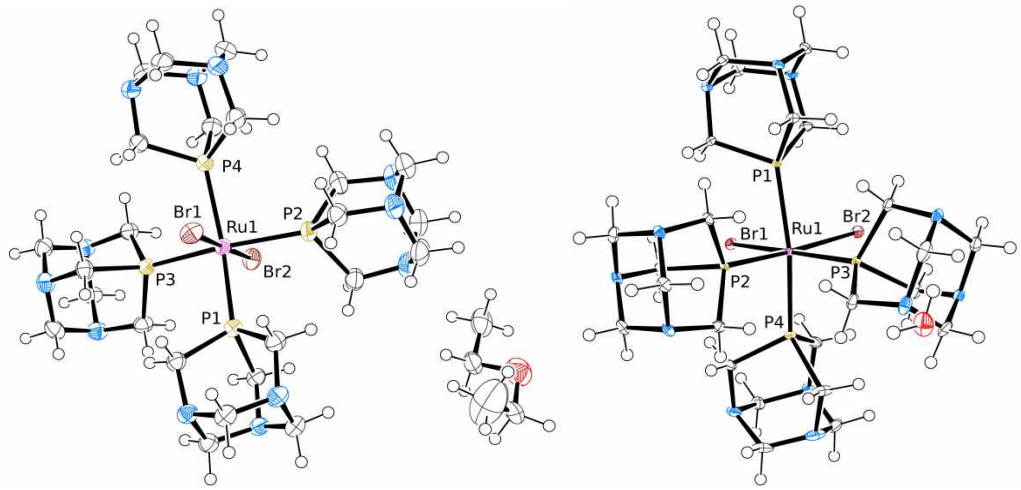

Figure 3. Molecular structures (50% probability ellipsoids) of *trans*-$[RuBr_2(PTA)_4]\cdot 0.682(C_4H_{10}O)$ (**3**, left) and *cis*-$[RuBr_2(PTA)_4]\cdot 0.37(H_2O)$ (**4**, right). The crystallization water molecule with minor occupancy factor in the structure of **3** has been omitted for clarity. Color code for unlabeled atoms: N = blue, O = red.

The molecular structures of **3** and **4** (Figure 3) are closely comparable with those of the corresponding dichloro derivatives [39-41]. To begin with, they show distortions from the perfect octahedral geometry around Ru(II) very similar to those found in **1** and **2**. In complex **3** the two pairs of *trans* PTA ligands are vertically displaced in opposite directions from the average equatorial plane (163.46(2) and 164.05(2)°). In complex **4** the two *trans* PTA ligands make a P–Ru–P angle of 164.639(18)° (164.8(1)° in **2**) and are bent towards the Br atoms. A similar bending is found for the two *cis* PTA's (97.067(19)° vs 96.5(1)° in **2**). Thus, in both isomers the PTA moieties move towards the less sterically encumbered region occupied by the two Br ligands. The two *trans* Ru–Br distances in **3** are nearly equal (2.5695(4) and 2.5582(4) Å) and slightly shorter than those found in the *cis* isomer **4** (2.6142(14) and 2.6289(4) Å), consistent with the stronger *trans* influence of PTA. Similarly, the Ru–P distances in the *trans* isomer range between 2.3253(7) and 2.3484(7) Å (cfr 2.316(2) – 2.353(2) Å in **1**), whereas in **4** the two Ru–P distances *trans* to Br are considerably shorter (2.2805(13) and 2.2655(5) Å; cfr 2.260(2) Å *trans* to Cl in **2**) than those of the two *trans* PTA's (2.4001(5) and 2.3562(5) Å; cfr 2.370(2) Å in **2**), which – in turn – are close to (but slightly longer than) those in the *trans* isomer.

The ^{1}H and ^{31}P NMR features of **3** and **4** and their chemical behavior in aqueous solution are also similar to those of the corresponding chloro compounds [39-42]. Whereas a light-protected D_2O solution of **3** is perfectly stable for days at room temperature according to NMR spectroscopy, the *cis* isomer **4** immediately equilibrates with the aqua species *cis*-$[RuBr(OH_2)(PTA)_4]^{+}$ and *cis*-$[Ru(OH_2)_2(PTA)_4]^{2+}$. Pure **4** – according to the ^{31}P NMR spectrum – was obtained only upon

addition of a large excess NaBr to the D_2O solution. This geometry-dependent behavior is in accordance with the trans influence of PTA observed in the X-ray structures. Consistent with literature data on Ru(II)-halide complexes, the bromide ligands proved to be more easily released than the chlorides [48]. An equilibrium constant of 2.42×10^{-2} M was measured between **4** and its mono-aqua derivative *cis*-$[RuBr(OH_2)(PTA)_4]^+$ by integration of the ^{31}P NMR signals (to be compared with 1.39×10^{-2} M for complex **2**). The measurement was performed in the presence of the minimum amount of NaBr sufficient to inhibit the formation of *cis*-$[Ru(OH_2)_2(PTA)_4]^{2+}$. The electronic absorption spectra of **1** and **3** in chloroform (SI) show a single band of low intensity in the visible region (λ_{max} = 452 nm for **1** and 475 nm for **3**), whereas those of the less symmetric *cis* isomers (SI) are characterized by a broad band, probably the overlap of two bands, at higher frequencies (λ_{max} = 348 nm for **2** and 368 nm for **4**). They are attributed to MLCT transitions from Ru(II) to the π-acceptor PTA, as in the corresponding Ru(II)–CH_3CN [48] and Ru(II)–dmso [49] compounds. Consistent with this assignment, the main absorption band of each Br isomer is red-shifted of ca. 20 nm compared to that of the corresponding Cl species (bromide, being a better π-donor than chloride, leads to an increase in the energy of the t_{2g} orbitals) [48]. The electronic absorption spectra of **2** and **4** in pure water and after addition of excess NaCl or NaBr are consistent with the NMR findings in D_2O (SI; see below the results in phosphate buffer).

The Ru(III) complex *trans*-$[RuCl_4(PTAH)_2]Cl$ (**5**) had been previously identified in very low yield upon recrystallization of **1** (to which a *cis* geometry had been wrongly assigned) in an aqueous HCl solution (the main product being the *bis*-protonated Ru(II) species *cis*-$[RuCl_2(PTA)_2(PTAH)_2]Cl_2$) [40]. Its origin – either a side product in the preparation of **1** due to incomplete Ru(III) reduction, or originated by adventitious air oxidation of **1** during the prolonged crystal growing experiments – was unclear. Even though neglected after the original report, we found complex **5** particularly exciting since it is structurally similar to the two best known Ru(III) anticancer drug candidates, namely NAMI-A and NKP-1339 (Figure 4) [1-10].

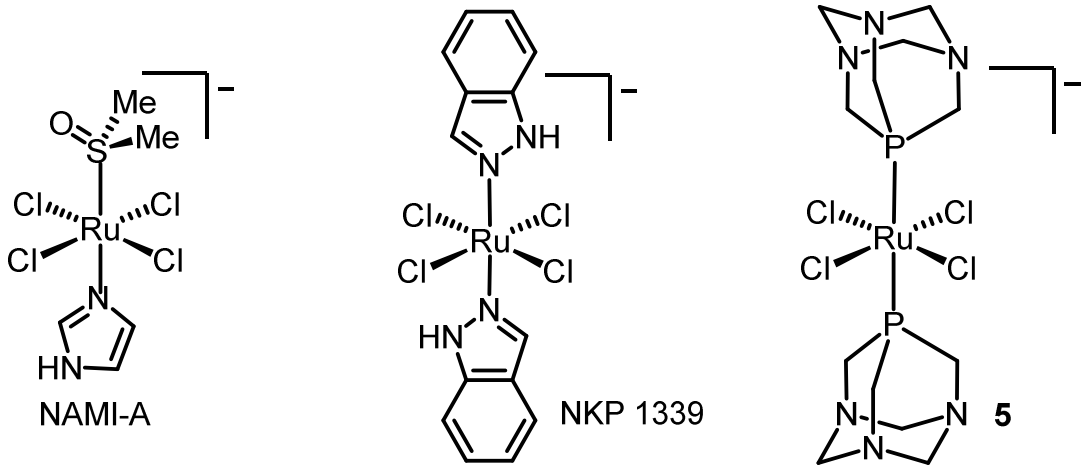

Figure 4. Comparison of the structurally related anions of the Ru(III) complexes NAMI-A (left), NKP-1339 (center) and **5** (represented in its anionic form with unprotonated PTA).

Interestingly, compound **5**, depending on the degree of protonation of the PTA ligands, can be cationic (*trans*-$[RuCl_4(PTAH)_2]^+$), neutral (*trans*-$[RuCl_4(PTA)(PTAH)]$), or anionic (*trans*-$[RuCl_4(PTA)_2]^-$). We found that **5** can be obtained in high yield upon treatment of the Ru(III)-dmso precursor $[(dmso)_2H]$*trans*-$[RuCl_4(dmso\text{-}S)_2]$ [43] with PTA in MeOH/HCl mixtures (Scheme 1). Due to the acidic conditions used in the preparation, both PTA ligands undergo protonation and the complex precipitates spontaneously in almost quantitative yield in its cationic form.

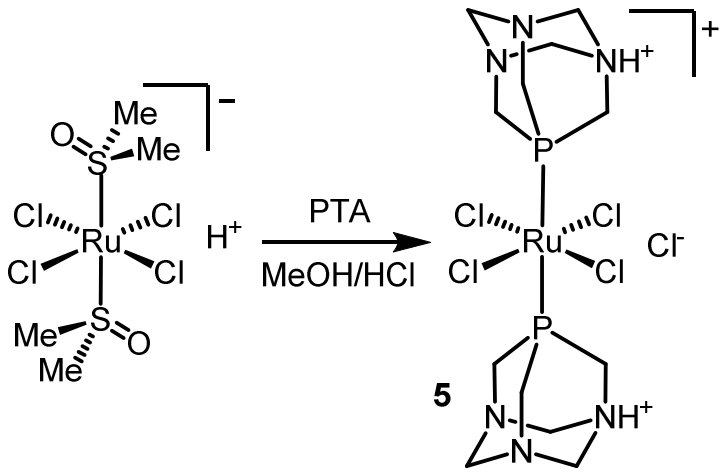

Scheme 1. Selective preparation of *trans*-$[RuCl_4(PTAH)_2]Cl$ (**5**) from the Ru(III)-dmso precursor $[(dmso)_2H]$*trans*-$[RuCl_4(dmso\text{-}S)_2]$.

Dark crystals of *trans*-$[RuCl_4(PTAH)_2]Cl\cdot H_2O$ (**5**$\cdot H_2O$) suitable for X-ray structure determination were obtained upon recrystallization of the raw product from water.

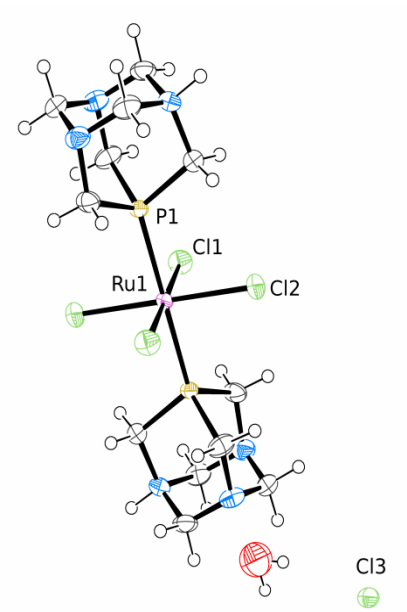

Figure 5. Molecular structure (50% probability ellipsoids) of *trans*-[$RuCl_4(PTAH)_2$]$Cl \cdot H_2O$ (**5**·H_2O). Only the chloride in the position of maximum occupancy is shown. Color code for unlabeled atoms: N = blue, O = red.

The molecular structure of complex **5** is in close agreement with that already published for this species [40]. One N atom in each PTA ligand is fully protonated, as confirmed by lengthening of the corresponding C–N bonds from 1.456(4) Å to 1.516(4) Å in the protonated form [27,28,38]. The positive charge of the complex is balanced by an external chloride ion that is disordered over three different positions.

The ^{1}H NMR spectrum of **5** in D_2O consists of two relatively broad peaks for bound PTA (one for the PCH_2N and the other for the NCH_2N protons) shifted upfield with respect to the typical PTA region (δ = 0.37 and –1.17 ppm, no assignment could be made). Consistent with the fact that P of PTA is directly bound to the paramagnetic Ru(III) nucleus, we were unable to observe any resonance in the ^{31}P NMR spectrum (most likely the expected singlet is too broad to be detected). The visible region of the absorption spectrum of **5** in water shows the typical halide-to-Ru(III) charge-transfer manifold typical of all Ru(III) complexes with a similar structure [43,48-50]: a main broad band centered at 383 nm and a weaker band at 444 nm (SI). The spectrum shows a very slow decrease of the band intensities (ca. –15 % in 72h at room temperature) without significant shifts in the absorption maxima (SI). Such spectral changes are not consistent with slow chloride release [43,48-50] (in fact, addition of excess NaCl after 72h induces no significant change in the spectrum), but rather suggest a progressive aggregation (and consequent decrease of the complex

concentration), perhaps involving species with different charge derived from the deprotonation equilibria of coordinated PTAH.

3.2 Spectrophotometric analysis.

The studied compounds display a remarkable solubility and a sufficient stability in water, thus being well amenable for biological studies. UV-vis absorption spectroscopy was chosen as the election method to monitor the behavior of the five complexes in a reference buffer at physiological pH over a time period of 24h. Time dependent spectral profiles for each compound are reported in Figure 6 (**1**-**4**) and Figure 7 (**5**).

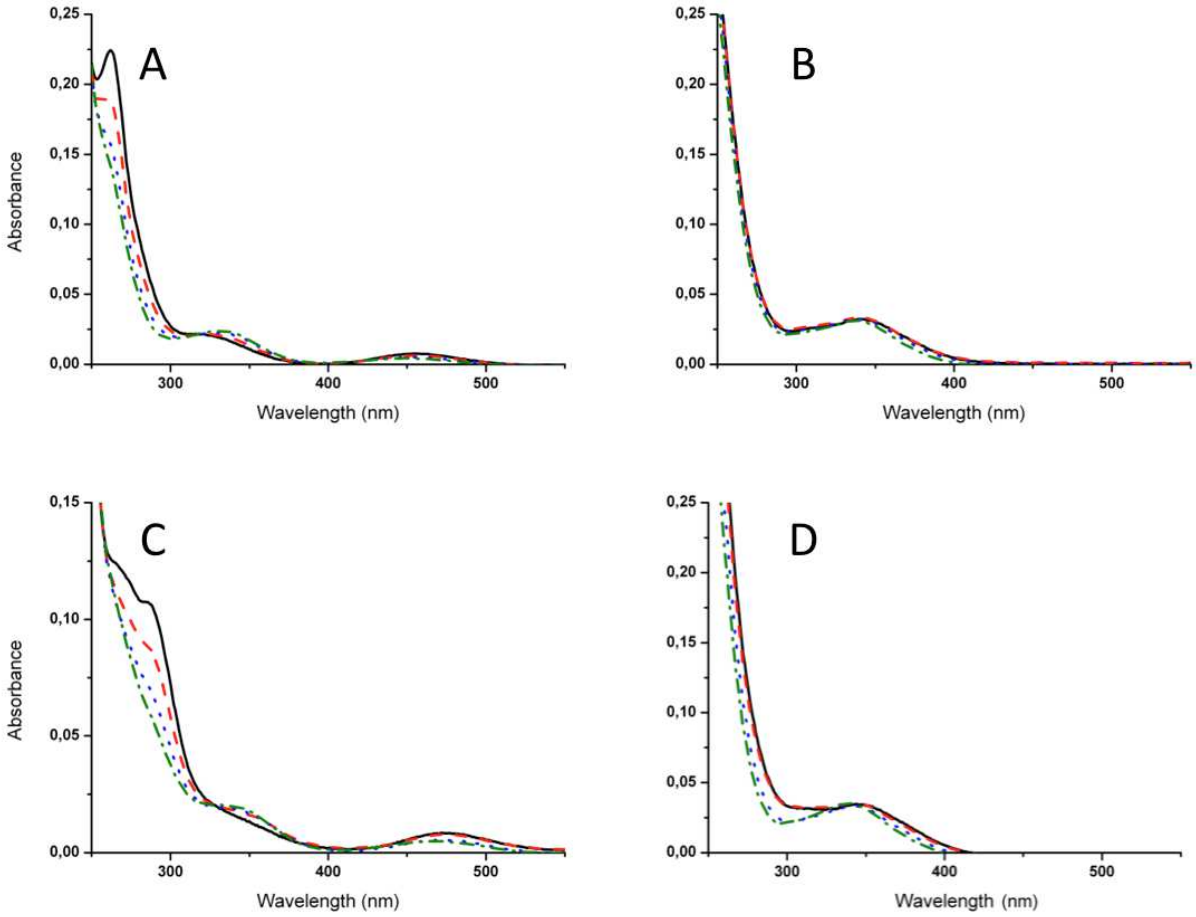

Figure 6. Time course UV-vis spectra of compounds **1** (A), **2** (B), **3** (C), and **4** (D) dissolved in 10 mM phosphate buffer, pH 7.4, over 1 hour. Figures show spectra recorded at t = 0 (black solid line), 10 min (red dashed line), 30 min (blue dotted line), and 1h (green dashed-dot line). (For interpretation of the references to color in this figure, the reader is referred to the web version of this article.)

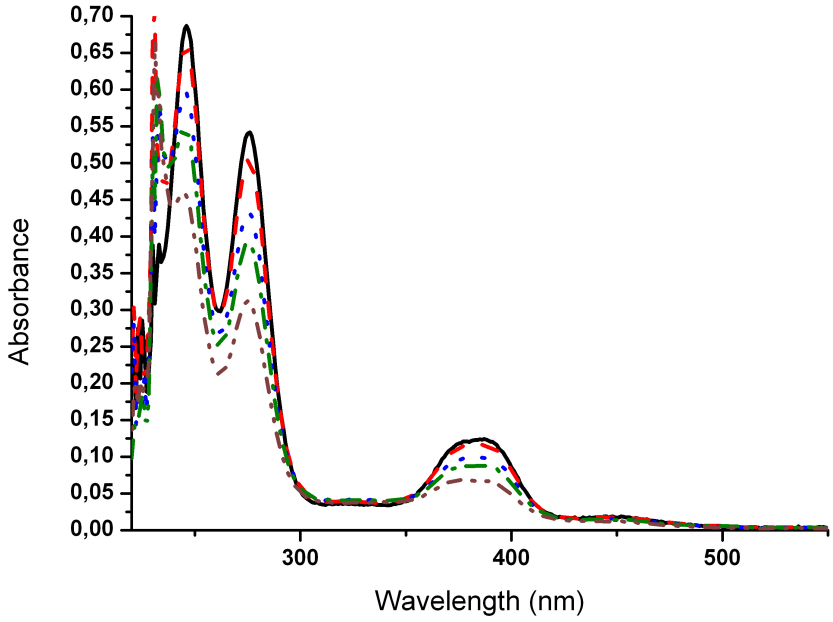

Figure 7. Time course UV-vis spectra of compound **5** dissolved in 10 mM phosphate buffer, pH 7.4, over 24 hours. Figures show spectra recorded at t = 0 (black solid line),1h (red dashed line), 6h (blue dotted line), 12h (green dashed-dot line), and 24h (brown dashed-dot-dot line). (For interpretation of the references to color in this figure, the reader is referred to the web version of this article.)

For the *trans* isomers **1** and **3**, contrary to what was observed by NMR spectroscopy in D_2O, where they are stable, spectral changes occurred within one hour (SI): for each complex the absorption band in the visible region (456 nm for **1** and 475 nm for **3**) progressively disappeared, whereas the band in the near UV region shifted to lower frequencies (325 nm for **1** and 344 nm for **3**). These spectral changes are ascribed to the progressive release of the halide ligands, even though concomitant partial release of PTA cannot be excluded. Conversely, the *cis* isomers **2** and **4** displayed a different behavior, similar to that found in pure water (SI): upon dissolution in the buffer both complexes showed a similar spectrum, with a band at 340 nm, whereas in chloroform solution compound **4** has a band which is red-shifted of ca. 20 nm compared to that of compound **2** (see above). In addition, the spectra in phosphate buffer showed no significant change with time, consistent with the NMR findings (in D_2O) that evidenced rapid equilibration of the *cis* isomers with the mono- and diaqua species upon release of the halide ligands. The aquation process, that is

expected to be more pronounced at the concentration used in the UV-vis spectra (compared to NMR), apparently leads to the common *cis*-$[Ru(OH_2)_2(PTA)_4]^{2+}$ species.

The spectrum of compound **5** changed with time in a manner similar (but faster) to that observed in pure water (see above) (Figure 7).

3.3 Reactions with model proteins.

The interactions of compounds **1-5** with the model proteins RNase and cyt c were subsequently monitored by ESI-MS analysis. Results are summarized in Figure 8 (interaction with cyt c) and in the SI (with RNase A). In general, as can be judged from the amount of the metallodrug-protein adducts that are formed, the reactivity is very limited, in particular with compound **5**. Nevertheless, careful analysis of ESI mass spectra allowed us to identify the metallic fragments that are bound to the proteins. In most cases mono-metalated derivatives are formed, in which the metallic fragment consists of the ruthenium center plus a variable number of PTA ligands. In particular, Figure 8 shows that in the case of cyt c the main peaks can be assigned to adducts bearing the fragments $[Ru(PTA)]^{2+}$, $[Ru(PTA)_2]^{2+}$ and $[Ru(PTA)_3]^{2+}$, respectively. In some cases fragments containing Cl^- or Br^- were also detected: $[RuCl(PTA)_2]^+$ for compound **1**, $[RuBr(PTA)_4]^+$ for compound **3**, $[RuBr(PTA)_3]^+$ for compound **4**, $[RuCl_3(PTAH)]^+$ and $[RuCl_4(PTAH)_2]^+$ for compound **5**. The interactions with RNase A (SI) lead to adducts that are similar to those obtained with cyt c. Moreover, adducts with $[RuCl]^+$ (for compounds **1** and **2**) and $[RuBr]^+$ (for compound **3** and **4**) were also detected.

Overall, the interactions detected between the model proteins and the five ruthenium complexes are rather modest, suggesting that proteins might not be primary and/or relevant targets.

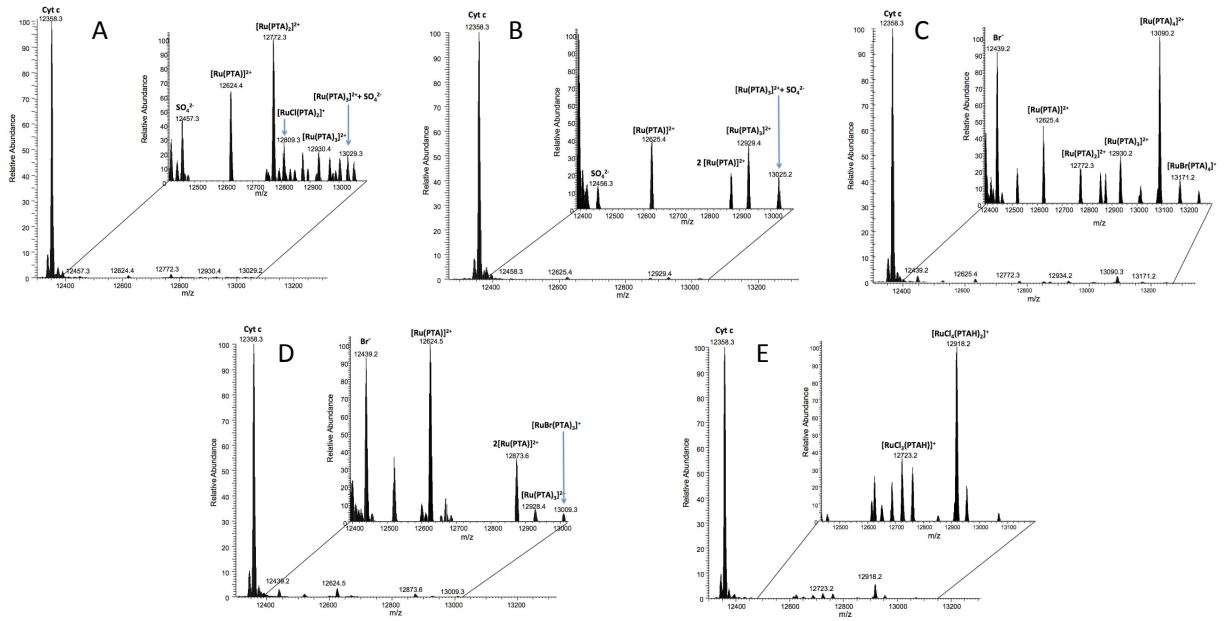

Figure. 8. LTQ Orbitrap ESI mass spectra of compound **1** (A), **2** (B), **3** (C), **4** (D) and **5** (E) dissolved in 20 mM ammonium acetate buffer, pH 7.4, in the presence of cyt c after 24h incubation at 37°C. The spectra in the back are the amplification of a region of the front spectra.

3.4 Reactions with a single strand oligonucleotide

The lack of relevant adduct formation with the selected model proteins, together with the evidence in literature that several Pt and Ru-based complexes may exert their biological effects through a direct interaction with DNA [51-53], prompted us to study the reactivity of the five ruthenium complexes with a DNA model system.

Investigations were performed on a single strand oligonucleotide, ODN4, (5'-CGCGCG-3'), chosen as reference, and the interactions were monitored through ESI-MS. In this case adduct formation was far more evident than with model proteins, with the exception of compound **5** (Figure 9). Adducts between the oligonucleotide and ruthenium fragments containing more than one PTA ligand were identified. Specifically, the main adduct between ODN4 and the *trans* isomers **1** and **3** (Figure 9A and C) contains the fragment $[Ru(PTA)_2]^{2+}$, whereas that with the *cis* isomers **2** and **4** (Figure 9B and D) bears $[Ru(PTA)_3]^{2+}$. Notably, even though compound **2** was reacted with ODN4 under the same conditions as the other ruthenium complexes, a drastic decay in the intensity of ESI-MS peaks was detected in this case, which might be tentatively ascribed to the occurrence of aggregation/precipitation processes. Nonetheless, a low intensity spectrum could be obtained (Figure 9B) and peak assignment was performed. It is worth mentioning that in this case the peak

relative to the free oligonucleotide was not detected after 24h incubation at 37°C, revealing that all the ODN4 has reacted. The only adduct that could be identified was that with the metallic fragment $[Ru(PTA)_3]^{2+}$.

In addition to the main adduct, ESI mass spectra of compounds **1** and **3** show peaks corresponding to derivatives: $2[Ru(PTA)_2]^{2+}$ and $[Ru(PTA)_2]^{2+}$+$[RuCl(PTA)_3]^{+}$ for compound **1**, $[Ru(PTA)_2]^{2+}$+$[RuBr(PTA)_3]^{+}$ and $2[RuBr(PTA)_3]^{+}$ for compound **3**. In the case of compound **4**, other mono- and bis-metalated adducts were also detected (i.e. $[Ru(PTA)_4]^{2+}$ and $2[RuBr(PTA)_3]^{+}$).

The interaction between more inert compound **5** and ODN4 is less evident and only small amounts of adducts could be detected. In fact, Figure 9E shows two peaks corresponding to the adducts between ODN4 and the fragments $[Ru(PTA)]^{3+}$ and $[Ru(PTA)_2]^{3+}$, while most of the free compound in solution is in the form $[RuCl_4(PTA)]^{-}$ or $[RuCl_4(PTA)_2]^{-}$ (SI).

It is evident that, in agreement with the NMR and UV-vis findings reported above, the two *cis* complexes (**2** and **4**) are more reactive than the respective *trans* species (**1** and **3**), and that the adduct formation is more evident with the chloride than with the bromide.

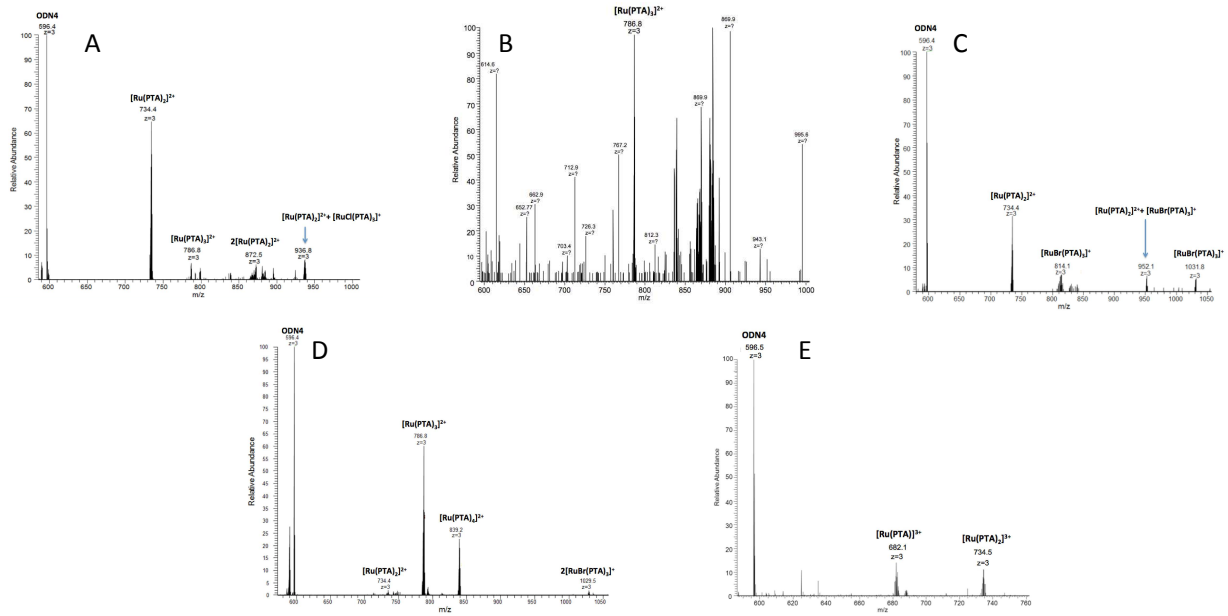

Figure 9. LTQ Orbitrap ESI mass spectra of compound **1** (A), **2** (B), **3** (C), **4** (D) and **5** (E) dissolved in milliQ water, in the presence of ODN4 after 24h incubation at 37°C.

3.5 Antiproliferative properties

The antiproliferative properties of compounds **1**-**5** were assessed against two cell lines: HCT-116 (human colon cancer) and FLG 29.1 (human acute myeloid leukemia) according to the method described in the experimental section. Both cell lines were treated for 24 hours with increasing concentrations of the drug and IC_{50} values determined (calculated through the Trypan blue exclusion test). The findings are summarized in Table 1. In general, the antiproliferative effects are quite moderate, yet the two *cis* isomers **2** and **4** were found to be significantly more effective than the *trans* congeners **1** and **3** in the leukemia cell line, whereas the cytotoxicity of compound **5** is far lower. It is also remarkable that the cytotoxic profile of **1** is virtually identical to that of **3**, and the same similarity was found for the two *cis* isomers **2** and **4**. This finding suggests that – in both cases – similar halide-free species are ultimately responsible for the biological effects. Such species are presumably different for the two stereoisomers because the activity clearly depends on the geometry of the complex. These results, together with the reactivity profiles toward the oligonucleotide, point out that the biological effects may be related to the direct interaction of these ruthenium compounds with DNA.

Table 1. IC_{50} values (μM) for compounds **1-5**, in comparison with cisplatin, on a solid tumor cell line, HCT 116, and a myeloid leukemia cell lines, FLG 29.1.

Compound	FLG 29.1	HCT 116
trans-$RuCl_2(PTA)_4$ (**1**)	>200	>100
cis-$RuCl_2(PTA)_4$ (**2**)	60.83 ± 0.59	>100
trans-$RuBr_2(PTA)_4$ (**3**)	>200	>100
cis-$RuBr_2(PTA)_4$ (**4**)	59.33 ± 0.41	>100
trans-$[RuCl_4(PTAH)_2]Cl\cdot 2H_2O$ (**5**)	84.91 ± 0.39	>100
Cisplatin	24.33 ± 0.75[a]	7.65 ± 0.63[b]

[a] From ref. 54. [b] From ref. 55.

4. Conclusions

The cage-like monodentate phosphine 1,3,5-triaza-7-phosphaadamantane (PTA) has been extensively used as co-ligand in many Ru half-sandwich anticancer compounds [11-26], where it plays a central role in increasing the aqueous solubility and in affecting the solution behavior [27,28]. However, no biological investigation has been yet performed on ruthenium complexes in

which PTA is the main ligand. With the aim of filling this gap, in this work we reported the preparation and characterization for prospective biomedical applications of a group of five ruthenium-PTA-halide compounds: the four structurally related Ru(II) complexes of general formula *trans*- or *cis*-$[Ru(PTA)_4X_2]$, X = Cl (**1**, **2**), Br (**3**, **4**)), and the Ru(III) compound *trans*-$[RuCl_4(PTAH)_2]Cl$ (**5**, PTAH = PTA protonated at one N atom).

The chemical behavior of the Ru(II) compounds in aqueous solution was found to depend on their structure and on the pH. In pure water, whereas the *trans* isomers **1** and **3** are very stable (in the dark), the *cis* analogues **2** and **4** readily equilibrate with the aqua species *cis*-$[RuX(OH_2)(PTA)_4]^+$ and *cis*-$[Ru(OH_2)_2(PTA)_4]^{2+}$. However, when dissolved in phosphate buffer at physiological pH, also the *trans* isomers undergo aquation processes that can be mainly ascribed to halide replacement. The reactivity of the four compounds with two model proteins, cytochrome c (cyt c) and ribonuclease A (RNase A), and with a DNA single strand reference oligonucleotide, ODN4 (5'-CGCGCG-3'), was investigated by mass spectrometry and their *in vitro* cytotoxicities against two representative cancer cell lines were also assessed. In general, compounds **1 - 4** showed a pairwise different – structure-related – behavior, clearly indicating that the four isomers do not converge to a common species but rather to two main halide-free stereoisomeric Ru-PTA fragments. Their reactivity towards cyt c and RNase A was found to be quite limited and minimal amounts of protein adducts were formed. Compounds **1** – **4** exhibited a far higher reactivity toward the reference oligonucleotide than toward model proteins and substantial amounts of adducts – mainly mono-ruthenated – are indeed formed where ruthenium fragments are coordinated to DNA nucleobases. The two *cis* isomers (**2** and **4**) turned out to be more reactive than the respective *trans* species (**1** and **3**). Finally, the four Ru(II) compounds manifested rather moderate antiproliferative properties against the two investigated cell lines: HCT-116 (human colon cancer) and FLG 29.1 (human acute myeloid leukemia). Consistent with the results described above, the *cis* isomers **2** and **4** were found to be significantly more effective than the *trans* congeners **1** and **3** in the leukemia cell line FLG 29.1.

The only investigated Ru(III) complex, **5**, deserves a separate comment. It was found to be very inert, both in pure water and in buffer, and basically unreactive towards the investigated biomolecules and devoid of any relevant cytotoxic activity towards the investigated cancer cell lines. Given the structural similarity between **5** and well known anticancer compounds KP-1019/NKP-1339 and NAMI-A, these findings were particularly disappointing. Nevertheless, they might suggest that for this type of anionic Ru(III) complexes, cytotoxicity is strictly related to the activation kinetics. Whereas the lack of cytotoxic activity of NAMI-A has been attributed to the fast

kinetics that lead to aquated Ru(III) metabolites unable to cross the cell membrane [56-57], the scarce activity of **5** might be attributed to exceedingly slow kinetics and to the consequential paucity of reactive aqua species. The intermediate activation kinetics (i.e. chloride release) of the more cytotoxic KP-1019/NKP-1339 complexes are apparently in the optimal range for observing *in vitro* activity.

Keywords: Ruthenium complexes; PTA; protein interaction; oligonucleotide interaction; in vitro antriproliferative activity

Highlights:

- Water-soluble Ru(II/III)-halide-PTA complexes (PTA = 1,3,5-triaza-7-phosphaadamantane)
- Structure and pH dependent solution behavior of the Ru(II)-PTA complexes.
- Evident interaction of such complexes with a single strand reference oligonucleotide
- Modest reactivity of the ruthenium compounds towards model proteins
- Structure dependent antiproliferative properties of the five ruthenium compounds

Abbreviations

Cyt c	Cytochrome c
ESI-MS	Electrospray ionization mass spectrometry
KP-1019	[indH]*trans*-[$RuCl_4(ind)_2$], ind = indazole
NAMI-A	[imH]*trans*-[$RuCl_4$(dmso-S)(im)], im = imidazole
NKP-1339	[Na]*trans*-[$RuCl_4(ind)_2$], ind = indazole
ODN	Oligodeoxyribonucleotide
PTA	1,3,5-triaza-7-phosphaadamantane
PTAH	PTA protonated at one N atom
RAPTA	Ruthenium-arene-PTA
RNase A	Ribonuclease A

Supporting Information

Electronic Supporting Information (SI) available: Essential crystal and refinement data, together with coordination bond distances and angles for **3**, **4** and **5**. ^{1}H, ^{31}P, and HSQC NMR spectra in $CDCl_3$ of *trans*-[$RuBr_2(PTA)_4$] (**3**) and *cis*-[$RuBr_2(PTA)_4$] (**4**); Experimental and calculated isotopic mass distribution for the $[M - Br]^+$ species; Inversion recovery ^{1}H NMR spectrum in D_2O of *trans*-[$RuCl_4(PTAH)_2$]Cl (**5**); UV-vis spectra of compounds **1** – **4** in $CHCl_3$; UV-vis spectra of compounds **2** and **4** in water (1.0 mM) immediately after dissolution, after 15 h at room temperature, and after addition of excess NaCl (**2**) or NaBr (**4**); UV-vis spectrum of compound **5** in water (0.4 mM) followed for 72 h at room temperature and after addition of excess NaCl; ESI mass spectra of compounds **1** - **5** after 24h incubation at 37°C with RNase A at pH 7.4; ESI mass spectrum of compound **5** after 24h incubation at 37°C with ODN4 in milliQ water. CCDC-1429123 (**3**), 1429111 (**4**), 1429110 (**5**).

Acknowledgments

We gratefully acknowledge Beneficentia Stiftung (Vaduz, Liechtenstein), the University of Trieste - FRA2013 (G. B. and E. A.), and EU COST CM1105 for financial support, Elena Michelucci, CISM (University of Florence) for recording ESI mass spectra and Dr. Carla Bazzicalupi (Department of Chemistry "Ugo Schiff", University of Florence for providing ODN4. Hydrated $RuCl_3$ was a generous gift from BASF Italia Srl.

References

[1] E. Alessio, G. Mestroni, A. Bergamo, G. Sava, Curr. Topics Med. Chem. 4 (2004) 1525-1535.

[2] Y. K. Yan, M. Melchart, A. Habtemariam, P. J. Sadler, Chem. Commun. (2005) 4764–4776.

[3] T. Gianferrara, I. Bratsos, E. Alessio, Dalton Trans. (2009) 7588-7598.

[4] A. Levina, A. Mitra, P. A. Lay, Metallomics 1 (2009) 458-470.

[5] C. G. Hartinger, P. J. Dyson, Chem. Soc. Rev. 38 (2009) 391-401.

[6] G. Süss-Fink, Dalton Trans. 39 (2010) 1673-1688.

[7] I. Bratsos, T. Gianferrara, E. Alessio, C. G. Hartinger, M. A. Jakupec, B. K. Keppler, in: E. Alessio (Ed.), Bioinorganic Medicinal Chemistry, Wiley-VCH, Weinheim, Germany, 2011, pp. 151-174.

[8] A. Bergamo, C. Gaiddon, J. H. M. Schellens, J. H. Beijnen, G. Sava, J. Inorg. Biochem. 106 (2012) 90-99.

[9] R. Trondl, P. Heffeter, C. R. Kowol, M. A. Jakupec, W. Berger, B. K. Keppler, Chem. Sci. 5 (2014), 2925-2932.

[10] C. Mari, V. Pierroz, S. Ferrari, G. Gasser, Chem. Sci. 6 (2015) 2660-2686.

[11] P. J. Dyson, G. Sava, Dalton Trans. (2006) 1929-1933.

[12] P. J. Dyson, Chimia 61 (2007) 698-703.

[13] C. Scolaro, A. Bergamo, L. Brescacin, R. Delfino, M. Cocchietto, G. Laurenczy, T. J. Geldbach, G. Sava, P. J. Dyson, J. Med. Chem. 48 (2005) 4161-4171.

[14] A. Bergamo, A. Masi, P. J. Dyson, G. Sava, Int. J. Oncol. 33 (2008) 1281-1289.

[15] W. H. Ang, A. Casini, G. Sava, P. J. Dyson, J. Organomet. Chem. 696 (2011) 989-998.

[16] C. M. Clavel, E. Paunescu, P. Nowak-Sliwinska, A. W. Griffioen, R. Scopelliti, P. J. Dyson, J. Med. Chem. 58 (2015) 3356-3365.

[17] M. V. Babak, S. M. Meier, K. V. M. Huber, J. Reynisson, A. A. Legin, M. A. Jakupec, A. Roller, A. Stukalov, M. Gridling, K. L. Bennett, J. Colinge, W. Berger, P. J. Dyson, G. Superti-Furga, B. K. Keppler, C. G. Hartinger, Chem. Sci. 6 (2015) 2449-2456.

[18] A. García-Fernández, J. Díez, Á. Manteca, J. Sánchez, R. García-Navas, B. G. Sierra, F. Mollinedo, M. Pilar Gamasa, E. Lastra, Dalton Trans. 39 (2010) 10186–10196.

[19] E. Menéndez-Pedregal, J. Díez, Á. Manteca, J. Sánchez, A. C. Bento, R. García-Navas, F. Mollinedo, M. Pilar Gamasa, E. Lastra, Dalton Trans. 42 (2013) 13955-13967.

[20] S. Seršen, J. Kljun, K. Kryeziu, R. Panchuk, B. Alte, W. Körner, P. Heffeter, W. Berger, I. Turel, J. Med. Chem. 58 (2015) 3984-3996.

[21] B. Serli, E. Zangrando, T. Gianferrara, C. Scolaro, P. J. Dyson, A. Bergamo, E. Alessio, Eur. J. Inorg. Chem. **(**2005) 3423-3434.

[22] D. N. Akbayeva, L. Gonsalvi, W. Oberhauser, M. Peruzzini, F. Vizza, P. Brueggeller, A. Romerosa, G. Sava, A. Bergamo, Chem. Commun. (2003) 264-.

[23] S. Grguric-Sipka, C. R. Kowol, S.-M. Valiahdi, R. Eichinger, M. A. Jakupec, A. Roller, S. Shova, V. B. Arion, B. K. Keppler, Eur. J. Inorg. Chem. (2007) 2870-2878.

[24] A. Romerosa, T. Campos-Malpartida, C. Lidrissi, M. Saoud, M. Serrano-Ruiz, M. Peruzzini, J. A. Garrido-Cárdenas, F. García-Maroto, Inorg. Chem. 45 (2006) 1289-1298.

[25] A. Romerosa, M. Saoud, T. Campos-Malpartida, C. Lidrissi, M. Serrano-Ruiz, M. Peruzzini, J. A. Garrido, F. García-Maroto, Eur. J. Inorg. Chem. (2007) 2803-2812.

[26] A. García-Fernández, J. Díez, Á. Manteca, J. Sánchez, M. Pilar Gamasa, E. Lastra, Polyhedron 27 (2008) 1214–1228.

[27] A. D. Phillips, L. Gonsalvi, A. Romerosa, F. Vizza, M. Peruzzini, Coord. Chem. Rev. 248 (2004) 955-993.

[28] J. Bravo, S. Bolaño, L. Gonsalvi, M. Peruzzini, Coord. Chem. Rev. 254 (2010) 555-607.

[29] D. J. Daigle, Inorg. Synth. 32 (1998) 40-45.

[30] P. Crochet, V. Cadierno, Dalton Trans. 43 (2014) 12447-12462.

[31] J. Kovács, T. Decuir Todd, J. H. Reibenspies, F. Joó, D. J. Darensbourg, Organometallics 19 (2000) 3963-3969.

[32] G. Laurenczy, F. Joó, L. Nádasdi, J. Elek, Chem. Commun. (1999) 971-972.

[33] G. Laurenczy, F. Joó, L. Nádasdi, Inorg. Chem., 39 (2000) 5083-5088.

[34] C. A. Mebi, R. P. Nair, B. J. Frost, Organometallics 26 (2007) 429-438.

[35] D. N. Akbayeva, L. Gonsalvi, W. Oberhauser, M. Peruzzini, F. Vizza, P. Brueggeller, A. Romerosa, G. Sava, A. Bergamo, Chem. Commun. (2003) 264-265.

[36] J. Kovács, F. Joó, A. Bényei, G. Laurenzy, Dalton Trans. (2004) 2336-2340.

[37] C. S. Allardyce, P. J. Dyson, D. J. Ellis, S. L. Heath, Chem. Commun. (2001) 1396-1397.

[38] Udvardy A, Bényei A. C., Kathó A, J. Organomet. Chem. 717 (2012) 116-122.

[39] D. J. Darensbourg, F. Joó, M. Kannisto,A. Katho, J. H. Reibenspies, Organometallics 11 (1992) 1990-1993.

[40] D. J. Darensbourg, F. Joó, M. Kannisto, A. Kathó, J. H. Reibenspies, D. J. Daigle, Inorg. Chem. 13 (1994) 200-208.

[41] C. A. Mebi, B. J. Frost, Inorg. Chem. 46 (2007) 7115-7120.

[42] R. Girotti, A. Romerosa, S. Mañas, M. Serrano-Ruiz, R. N. Perutz, Inorg. Chem. 48 (2009) 3692-3698.

[43] E. Alessio, G. Balducci, M. Calligaris, G. Costa, W. M. Attia, G. Mestroni, Inorg. Chem. 48 (1991) 609-618.

[44] W. Kabsch, Acta Cryst. D 66 (2010) 125-132.

[45] M. C. Burla, R. Caliandro, B. Carrozzini, G. L. Cascarano, C. Cuocci, C. Giacovazzo, M. Mallamo, A. Mazzone, G. Polidori, J. Appl. Cryst. 48 (2015) 306-309.

[46] G. M. Sheldrick, Acta Cryst. 64 (2008) 112-122.

[47] P. Emsley, K. Cowtan, Acta Cryst. D 60 (2004) 2126-2132.

[48] C. M. Duff, G. A. Heath, J. Chem. Soc. Dalton Trans. (1991) 2401-2411.

[49] E. Alessio, Chem. Rev. 104 (2004) 4203-4242.

[50] E. Alessio, G. Balducci, A. Lutman, G. Mestroni, M. Calligaris, W. M. Attia, Inorg. Chim. Acta 203 (1993) 205-217.

[51] R. Elizabeth, J. Lippard, S. J. Lippard, Chem. Rev. 99 (1999), 2467−2498.

[52] E. Gallori, C. Vettori, E. Alessio, F. G. Vilchez, R. Vilaplana, P. Orioli, A. Casini, L. Messori, Arch. Biochem. Biophys. 376 (2000) 156-162.

[53] D. Musumeci, L. Rozza, A. Merlino, L. Paduano, T. Marzo, L. Massai, L. Messori, D. Montesarchio, Dalton. Trans. 44 (2015) 13914-13925.

[54] T. Marzo, G. Bartoli, C. Gabbiani, G. Pescitelli, S. Pillozzi, E. Michelucci, B. Fiorini, A. Arcangeli, A. G. Quiroga and L. Messori; submitted manuscript.

[55] T. Marzo, S. Pillozzi, O. Hrabina, J. Kasparkova, V. Brabec, A. Arcangeli, G. Bartoli, M. Severi, A. Lunghi, F. Totti, C. Gabbiani, A. G. Quiroga, L. Messori, Dalton Trans. 44 (2015) 14896-14905.

[56] A. Levina, A. Mitra P. A. Lay, Metallomics. 1 (2009) 458-470.

[57] J. B. Aitken, S. Antony, C. M. Weekley, B. Lai, L. Spiccia, H. H. Harris, Metallomics, 4 (2012) 1051-1056.

Synopsis

This work reports the preparation and characterization of five water-soluble Ru(II)- and Ru(III)-halide-PTA (PTA = 1,3,5-triaza-7-phosphaadamantane) complexes. The structure and pH dependent solution behavior of the compounds, their interactions with model proteins and with a single strand reference oligonucleotide, and their antiproliferative properties are discussed in comparison with established ruthenium drug candidates in clinical development.